Molecular Structure of Tetrakis(*tert*-butylimido)osmium(VIII), determined in the Gas Phase by Electron Diffraction†

David W. H. Rankin,*[a] Heather E. Robertson,[a] Andreas A. Danopoulos,[b] Paul D. Lyne,[b] D. Michael P. Mingos[b] and Geoffrey Wilkinson*[b]

[a] *Department of Chemistry, The University of Edinburgh, West Mains Road, Edinburgh EH9 3JJ, UK*

[b] *Johnson-Matthey Laboratory, Chemistry Department, Imperial College of Science, Technology and Medicine, London SW7 2AY, UK*

The molecular structure of $Os(NBu^t)_4$ has been determined in the gas phase by electron diffraction. The NBu^t groups are in a distorted-tetrahedral arrangement around the central osmium atom, and bent in such a way that the overall molecular symmetry is reduced to S_4. The Os–N bond length (r_a) is 175.0(3) pm, and Os–N–C is 156.4(15)°. Two of the N–Os–N angles (about the S_4 axis) are 104.6(14)° and the other four are 111.9(7)°. Other important parameters are r(N–C) 147.6(9), r(C–C) 152.7(4) pm and N–C–C 107.0(5)°. Geometrical parameters for $Os(NMe)_4$ and $Os(NH)_4$ optimised using density functional theory are presented, and interpreted with the aid of extended-Hückel calculations.

Terminal alkylimido ligands in transition-metal complexes may be either linear or bent at nitrogen. In the linear examples the metal–nitrogen bond is regarded formally as being a triple bond and the nitrogen is a four-electron donor, whereas in the bent examples there is a double M=N bond and the nitrogen donates two electrons. In many cases, structures have been rationalised in terms of the 18-electron rule. For example, in $Os(NBu^t)_2O_2$[1] one ligand is linear at nitrogen [the angle is 178.9(9)°] whereas the other one is bent, with an angle of 155.1(8)°. The oxygen atoms and one of the imido ligands are taken as being two-electron donors, while the second imido ligand is a four-electron donor, giving the osmium a total of 18 electrons. However, in many other examples, the situation is not nearly so clear-cut, and observed angles cover the whole range from 150 to 180°. Moreover, there is no simple correlation between angles at nitrogen and metal–nitrogen bond lengths.

We have recently described the synthesis and some reactions of $Os(NBu^t)_4$ **1**,[2,3] the first homoleptic alkylimido complex of osmium(VIII). We have been unable to obtain structural data in the solid phase because **1** is a low-melting solid (m.p. ≈ 300 K), which when cooled slowly below its melting point crystallises as irregular small plates. However, in view of its high volatility in vacuum and relatively high symmetry, it seemed a good candidate for electron diffraction study in the gas phase. In this paper we report the results of this study. Details of the geometries of $Os(NMe)_4$ and $Os(NH)_4$, optimised using density functional theory, are also presented and interpreted with the aid of extended-Hückel calculations.

Experimental

A sample of compound **1** was synthesised by the reaction of OsO_4 with $NHBu^t(SiMe_3)$, as reported before.[2] Electron diffraction data were recorded photographically on Kodak Electron Image plates using the Edinburgh gas diffraction apparatus,[4] operated at 44.5 kV. The sample was held at 366 K and the inlet nozzle at 384 K during the diffraction experiments. Three plates were exposed at each of three camera distances, 95, 200 and 259 mm. It proved to be very difficult indeed to get satisfactory data, as the sample had a rather low vapour pressure under the experimental conditions, but was close to its decomposition temperature. Moreover, the amplitudes of the intensity oscillations attributable to the Os–N and Os···C contributions to the scattering fall to zero at around s = 120 nm^{-1}, and consequently the patterns on middle and short camera-distance plates were more or less featureless. The best plates, two exposed at the short camera distance, three at the middle distance and one at the long distance, were selected and optical densities recorded on a Joyce-Loebl MDM6 microdensitometer at the SERC Daresbury Laboratory.[5] The scanning,[5] data-reduction,[5] and least-squares refinements[6] were performed using standard programs and the scattering factors calculated by Fink and co-workers.[7] The electron wavelength was calibrated using scattering data from benzene, recorded concurrently with those for the osmium complex. The wavelengths are listed, with other relevant experimental parameters, in Table 1.

† *Non-SI unit employed*: eV ≈ 1.60 × 10^{-19} J.

Structural Analysis

Molecular Model.—Even if some of the ligands are two-electron donors and others donate four electrons, the four ligands would be expected to be identical, by what can be described as resonance. For the least-squares analyses of the diffraction data it was therefore assumed that the four butylimido groups were identical, each having C_3 local symmetry. Their geometry was defined by N–C, C–C and C–H bond lengths, N–C–C and C–C–H angles, and the twist angle for the methyl groups, away from the staggered position. The positions of the butylimido groups relative to the osmium atom were defined by the Os–N bond length, the Os–N–C angle and the torsion angle about the N–C bond; the zero position for this last parameter was defined to be that in which one C–C bond was *anti* to the Os–N bond. Finally, the overall molecular symmetry was allowed to be S_4 or D_2, with the N–Os–N angle about the C_2 axis and the torsion angle about the Os–N bonds as refinable parameters. The zero torsion angle was defined to correspond to the staggered conformation, for which the molecular symmetry of the $Os(NC)_4$ fragment was D_{2d}.

Least-squares Refinements.—The radial distribution curve (Fig. 1) reveals the major features of the structure of $Os(NBu^t)_4$, but care must be taken in its interpretation. The complex scattering factors used in electron diffraction studies are such that the distance between a heavy atom and a light one is

Table 1 Experimental conditions, data ranges, *etc.*[a]

Camera height/ mm	Δs / nm^{-1}	s_{min}	sw_1	sw_2	s_{max}	Correlation parameter[b]	Scale factor[b]	Wavelength/ pm
258.59	2	20	40	140	164	0.410	0.942(25)	5.672
199.76	4	40	60	192	224	0.155	0.736(16)	5.669
94.87[c]	4	112	132	280	308	−0.126	0.772(49)	5.674

[a] See ref. 6 for precise definitions of terms in column headings. [b] Refinement A. [c] Not included in refinement B.

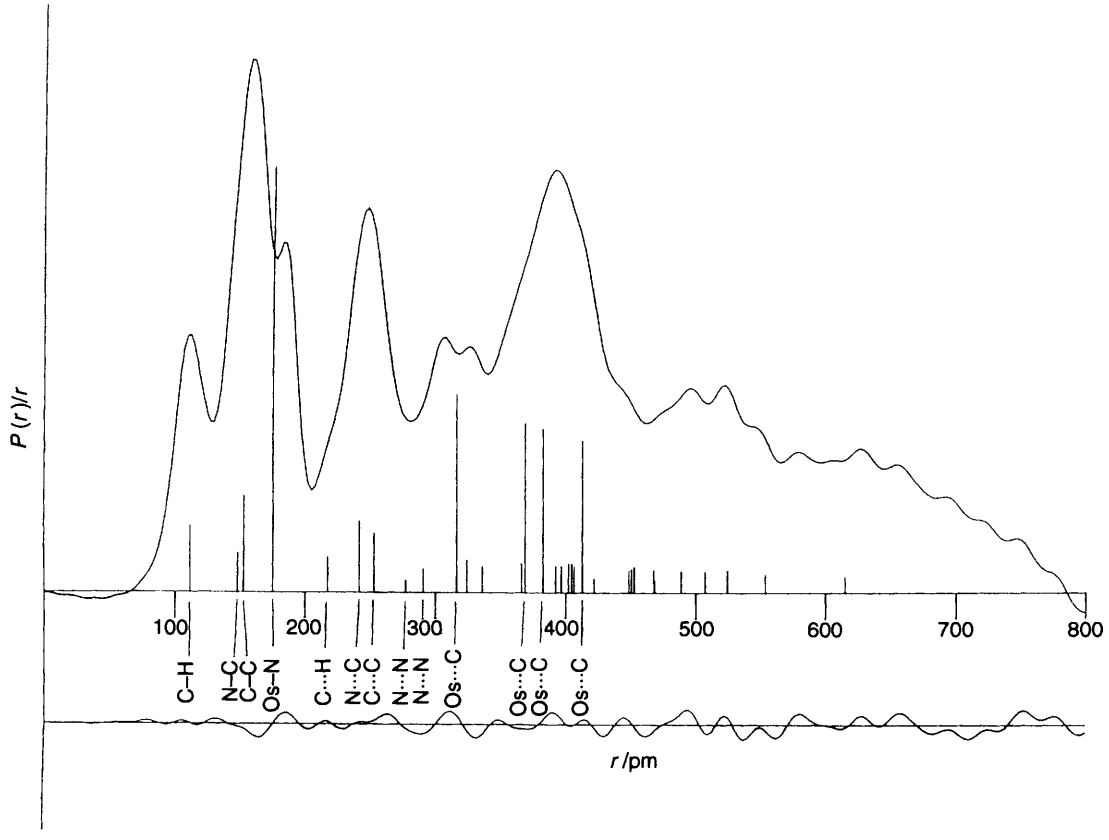

Fig. 1 Radial distribution curve for $Os(NBu^t)_4$. Before Fourier inversion the data were multiplied by $s\cdot\exp(-0.00003s^2)/(Z_{Os} - f_{Os})(Z_C - f_C)$. The difference curve (experimental − theoretical) corresponds to refinement A

represented by *two* peaks in the radial distribution curve, the interatomic distance corresponding to the minimum between the peaks. This is very clearly illustrated by a study of OsO_4.[8] In the present case, the non-bonded Os ··· C distance at 315 pm gives an obvious split peak with maxima at *ca.* 305 and 325 pm. There is a similar splitting of the Os–N peak at 175 pm, but the lower component overlaps a large peak, attributable to C–C and C–N bonds, and so only the upper component, at *ca.* 185 pm, is fully resolved. Other major peaks are C–H at 110 pm, non-bonded C ··· C and C ··· N at *ca.* 250 pm, and a broad and complex feature between 370 and 420 pm, which contains three distinct Os ··· C(methyl) components.

The data can only be fitted by assuming that the ligands are substantially bent at nitrogen. The Os–N–C angle refined to about 156° and differed from 180° by more than 16 standard deviations. This angle is well determined primarily because the Os–N and Os ··· C peaks are intense and isolated in the radial distribution curve, and the position of the Os ··· C peak makes it certain that the ligands cannot be linear, at least in the r_a structure. The breadth of the Os ··· C(methyl) peak at 370–420 pm supports this interpretation, as the three Os ··· C separations would be equal for linear ligands. However, it is always possible that the structure at the potential minimum includes linear ligands, and that the apparent non-linearity is a shrinkage effect. Unfortunately, it is impossible to determine a reliable force field, from which shrinkage corrections could be calculated, for a molecule of this complexity, containing a heavy metal atom. We therefore cannot state definitely that this molecule contains non-linear ligands in its configuration at the potential minimum, but it should be noted that the linear arrangement, with a very large-amplitude bending motion leading to a large shrinkage effect, is not that different from a non-linear arrangement: in neither case does the potential energy rise steeply on bending, falling a little in one case and rising a little in the other.

There are sufficient resolved features in the radial distribution curve to allow refinement of all the major parameters, although the N–C and C–C bond lengths were correlated (Table 2). Information about torsion angles, the configuration of the ligands at the osmium atom, and thus the overall molecular symmetry, is contained in the complex tail of the radial distribution curve, which covers the region from 400 to 800 pm and contains about 200 different contributing peaks. The whole range of possible conformations was investigated by setting the torsion angles at various fixed values, and setting the molecular symmetry to S_4 or D_2. The structure was then set at the geometry fitting the data best (which had S_4 symmetry) and the torsion angles were allowed to refine. Subsequently the Os–N

Table 2 Least-squares correlation matrix (× 100) for refinement A

p_2	p_3	p_4	p_5	p_6	p_7	p_8	p_9	p_{10}	u_1	u_2	u_5	u_{10}	u_{11}	u_{12}	u_{13}	k_1	k_2	k_3	
−14	23	0	4	−7	17	12	−10	17	−9	−39	2	0	7	5	−5	4	−1	−2	p_1
	−75	−4	−55	−63	−58	29	3	−2	−3	42	8	−16	−41	−65	1	−14	−4	0	p_2
		8	50	45	45	−18	16	12	12	−37	−1	10	31	50	−3	8	0	4	p_3
			5	8	0	−25	6	−3	4	−1	0	1	1	3	0	4	1	0	p_4
				74	26	−18	11	2	2	−23	−13	−1	39	66	−14	10	2	−1	p_5
					18	−32	−8	−13	5	−19	−8	−1	53	67	−7	15	7	3	p_6
						11	−16	19	−14	−38	−18	11	35	47	−4	−11	−9	−19	p_7
							2	16	5	10	0	1	−5	−18	1	−24	−10	9	p_8
								11	12	7	25	−27	−16	−22	−11	4	−4	9	p_9
									−1	−8	−4	18	−24	15	6	−2	−4	−2	p_{10}
										56	25	4	−1	0	4	10	18	74	u_1
											18	−3	−18	−27	4	4	16	52	u_2
												−14	−12	−23	−2	3	6	30	u_5
													1	17	44	7	2	5	u_{10}
														66	−51	16	0	−3	u_{11}
															−18	20	3	−4	u_{12}
																−1	3	6	u_{13}
																	−22	10	k_1
																		18	k_2

p_n is the nth parameter in Table 3, u_n is the amplitude of vibration for distance n in Table 4, and k_n is the scale factor for data set n in Table 1.

twist refined in the range 0–10°, with an estimated standard deviation (e.s.d.) of between 4 and 6°, so it was then fixed, at −0.8°, the value at which it settled in the last refinement in which it was included. The other twist angles refined satisfactorily, although their standard deviations were 3 or 4°. Amplitudes of vibration which were not included in the final refinement were fixed at values determined for related molecules. In a few cases amplitudes were refined in the early stages, but were subsequently fixed if their standard deviations were very large. In these cases the amplitudes were left at their refined values, if these were within one standard deviation of the expected value.

The significance of the observed distortion from regular, tetrahedral co-ordination was then tested. The N–Os–N angle parameter was fixed at 109.47°, thus making all N–Os–N angles equal, and all other parameters were refined as before. The R factor rose from 0.117 to 0.148, so the hypothesis that there is no distortion can be rejected with more than 99.5% confidence. This is also supported by the result of the refinements listed in Table 3, which show the refined angle, N(2)–Os–N(16), to differ from the tetrahedral angle by just over three standard deviations. The possibility that the molecule can be fitted by a model having T_d or T symmetry can be rejected, as the Os–N–C angle differs from 180° by 16 standard deviations.

It has been noted[9] that theoretical phase parameters for heavy atoms do not reproduce the experimental 'beat-out' position in the scattering data very precisely, but that the fit can be improved by replacing the parameters with those calculated for an atom of slightly different atomic number. Refinements were performed using theoretical[7] phase parameters for elements with atomic numbers in the range 72–82. The optimum fit was obtained using the tungsten (Z = 74) parameters, and these were used in subsequent refinements. Since the major components of the scattering beat out at *ca.* s = 120 nm^{-1}, the total molecular scattering at high angles is relatively weak, and consequently the R factor is correspondingly high. We therefore performed two final refinements. In refinement A data collected at all three camera distances were used. As this included short-distance (wide-angle) data, the R factor (R_G) was high (0.208) compared with that from refinement B, in which the short-distance data were excluded, giving an R factor of 0.117. Nevertheless, the standard deviations for most parameters in refinement A are smaller than those in B, and the preferred set of parameters is therefore those of A.

The difference scattering and radial distribution curves, Figs. 1 and 2, show considerable noise. This cannot be avoided, due to extreme experimental difficulties outlined in the Experimental section. However, the differences do appear to be random noise, and show no systematic errors. The effects of the noise are, of course, taken into account in the calculation of standard deviations, and the results reported are therefore those which are consistent with the data.

Table 3 Geometrical parameters (distances/pm, angles/°)[a]

		Refinement A	Refinement B
p_1	r(Os–N)	175.0(3)	175.9(5)
p_2	r(N–C)	147.6(9)	147.6(8)
p_3	r(C–C)	152.7(4)	152.9(4)
p_4	r(C–H)	111.1(4)	111.6(3)
p_5	Angle N(2)–Os–N(16)	104.6(14)	104.8(15)
p_6	Angle Os–N–C	156.4(15)	156.1(13)
p_7	Angle N–C–C	107.0(5)	107.2(5)
p_8	Angle C–C–H	109.9(15)	109.4(16)
p_9	Methyl twist[b]	23.4(35)	21.6(30)
p_{10}	Butyl twist[b]	43.0(38)	44.8(30)
p_{11}	Os–N twist[b]	−0.8[c]	−0.8[c]

[a] Parameters correspond to the r_a structure. Estimated standard deviations (in parentheses) were obtained in the least-squares refinements. [b] For definition see text. [c] Fixed.

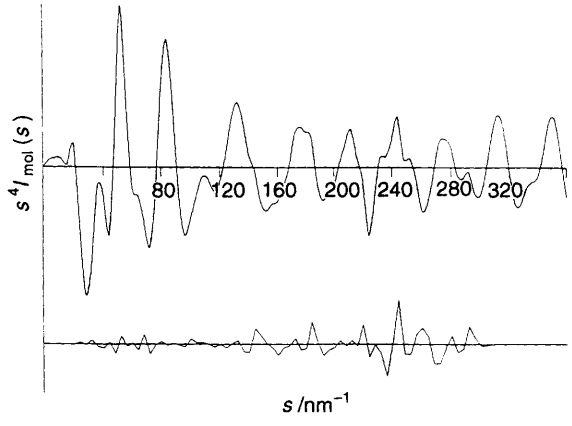

Fig. 2 The combined experimental and final weighted difference molecular scattering intensity curves for refinement A of the structure of Os(NBu^t)$_4$. Theoretical data have been included for those regions (below s = 20 and above s = 308 nm^{-1}) for which no experimental data are available

There are no interatomic distances above 800 pm, so the radial distribution curve is shown only to that limit. If it is plotted beyond that point it becomes negative, but the difference curve remains level. This is an artefact of the numerical method used for Fourier transformation, and arises from the s interval used. In fact, the envelope of the curve transforms into a point in the intensity curve which lies below $s = \Delta s$, and which therefore cannot be represented by either the theoretical or experimental data.

The final geometrical parameters, interatomic distances and amplitudes of vibration for both refinements are given in Tables 3 and 4 respectively. Fig. 2 shows the combined experimental scattering intensities and final difference curve for refinement A, and Fig. 3 contains a perspective view of the molecule and a projection along the C_2 axis.

Discussion

An alkylimido ligand is potentially a two- or four-electron donor, using the radical method of electron counting. When the ligand bridges two or three metal atoms it normally contributes four electrons for metal–nitrogen bond formation, but when it is terminal it may contribute either two or four, depending on whether it is bent or linear at nitrogen. Terminal imido groups are usually considered to be effectively linear if the M–N–C angle is greater than 170°, and bent if it is in the range 140–165°,

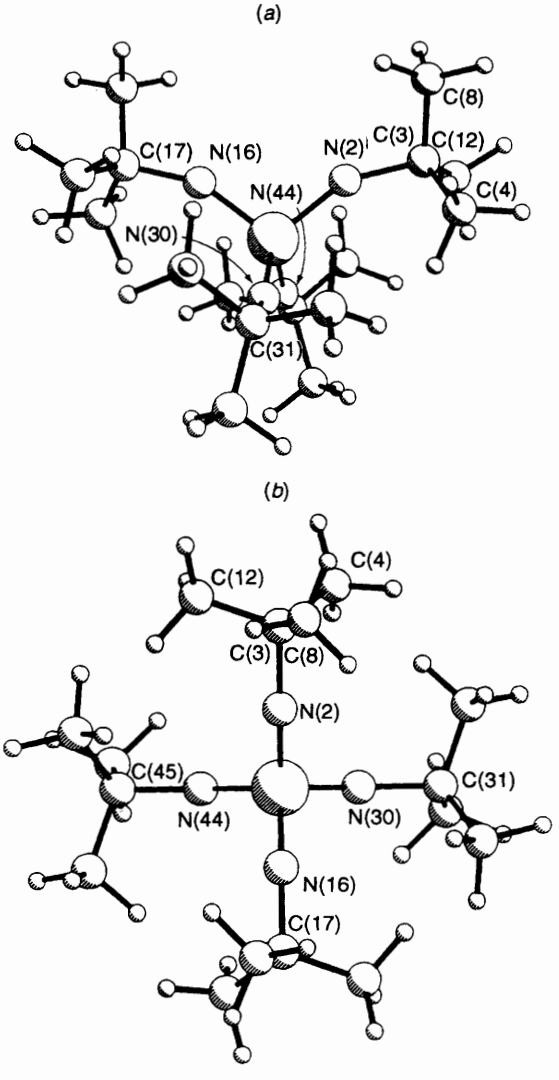

Fig. 3 A perspective view (*a*) and a projection along the C_2 axis (*b*) of $Os(NBu^t)_4$. In (*a*) the C_2 axis runs from top to bottom, in the plane of the paper

but there is no clear-cut distinction, and angles between 165 and 170° may be interpreted either way.[10] Note that observed angles never approach 125°, which is normally expected for an imine, $R_2C{=}NR$, suggesting that the bonding in bent and linear complexes may not be very different.

It has been suggested[11] that bending in imido ligands occurs to maintain an 18-electron count in electron-rich compounds with strong π donors (*e.g.* imido, amido or alkoxy) as coligands. Bent imido groups, having a lone pair of electrons, exhibit nucleophilic reactivity, and as $Os(NBu^t)_4$ does behave as a nucleophile the observed Os–N–C angle of 156.4(15)° is not surprising. In Table 5 some geometrical data for the simple osmium(VIII) complexes containing only oxo and/or *tert*-butylimido ligands are presented. Unfortunately, there are no data available for $Os(NBu^t)_3O$, although this compound is known.[10] There is a progressive shortening in the Os–N bond lengths as the number of imido ligands decreases, and this has been ascribed to decreasing competition for vacant osmium d orbitals by filled nitrogen orbitals. However, this competition also involves filled orbitals on the oxygen atoms, and there is no evidence for a corresponding increase in Os–O bond lengths as the imido ligands are replaced by oxygen.

An alternative approach makes use of the fact that one ligand is required to donate four electrons for osmium to reach a total of 18 electrons. In the case of $Os(NBu^t)O_3$[12] it must be the imido ligand which provides the four electrons, as it is linear at nitrogen, and so the Os–N bond must be a triple bond. At the other extreme of the series only one of the four ligands in $Os(NBu^t)_4$ needs to donate four electrons. The observed structure may therefore be regarded as representing an average of one Os–N triple bond and three double bonds, with a correspondingly greater average bond length. The two remaining compounds would be expected to have intermediate bond lengths. This is certainly true for $Os(NBu^t)_2O_2$, but this does present another problem: one of its imido ligands is almost linear and the other is bent, as expected, but the two Os–N bonds are not significantly different in length, whereas we would expect one to be a triple bond, *ca.* 169 pm long, while the other would be a double bond, *ca.* 176 pm long.

This raises the question of whether there really is any correlation between bond length and angle in alkylimido complexes. Fig. 4 shows the distribution of observed bond lengths and angles in rhenium, tungsten and osmium *tert*-butylimido complexes, with corrections made for the different sizes of the metal atoms. There is certainly no unequivocal correlation of bond length with angle. This may be because the quoted errors in parameters are actually smaller than the true errors, or it may be that there are systematic causes of variation, such as the co-ordination number or oxidation state of the metal, or the effects of the other ligands, which may influence the σ overlap of metal and nitrogen orbitals. If the two obviously out-lying points are ignored, the best-fit straight line is given by r(Os–N) = 202.1 − 0.1922 angle (Os–N–C). This gives 167.5 pm for the Os–N distance in a linear arrangement, and 172.3 pm in a typical bent ligand with an angle of 155°. However, the root mean square (r.m.s.) deviation in the fit to the bond lengths only rises from 3.5 to 3.6 pm if it is assumed that the Os–N distance is independent of the Os–N–C angle, so the evidence for any correlation is tenuous.

It is important to remember that although each electron interacts with a molecule only for about 10^{-19} s, the total diffraction pattern is derived from the ensemble of vibrational states and instantaneous structures present in the gas at the temperature of the experiment. We must consider what would be observed if the structure at the potential-energy minimum did in fact have one linear and three bent imido ligands. Extended-Hückel calculations[1] on $Os(NBu^t)_2O_2$ and $Os(NMe)_2O_2$ have shown that there is a potential-energy maximum for the linear configuration of the ligands, but that this is only *ca.* 4 kJ mol^{-1} above the energy for the most stable, bent arrangement. (The angles at the minima are not given.)

Table 4 Interatomic distances and amplitudes of vibration[a]

		Refinement A		Refinement B	
		Distance/pm	Amplitude/pm	Distance/pm	Amplitude/pm
r_1	Os–N	175.0(3)	3.4(6)	175.9(5)	3.3(14)
r_2	N–C	147.6(9)	6.0(7)	147.6(8)	5.9(6)
r_3	C–C	152.7(4)		152.9(4)	
r_4	C–H	111.1(4)	6.2[b]	111.6(3)	6.2[b]
r_5	Os · · · C	315.9(6)	5.3(8)	316.5(11)	4.1(19)
r_6	N(2) · · · N(16)	277.0(18)	8.0[b]	278.7(22)	8.0[b]
r_7	N(2) · · · N(30)	290.1(9)	8.0[b]	291.5(10)	8.0[b]
r_8	N(2) · · · C(4)	241.4(5)	7.0[b]	241.9(6)	7.0[b]
r_9	C(4) · · · C(8)	252.9(6)	7.0[b]	252.9(6)	7.0[b]
r_{10}	Os · · · C(4)	368.3(16)	8.5(16)	369.7(18)	8.2(34)
r_{11}	Os · · · C(8)	412.5(10)	13.7(41)	414.2(11)	15.1(35)
r_{12}	Os · · · C(12)	382.1(14)	12.1(39)	382.3(12)	12.6(38)
r_{13}	N(2) · · · C(17)	421.8(15)	9.0(29)	423.5(23)	7.3(36)
r_{14}	N(2) · · · C(31)	400.9(9)		401.9(10)	

The uncertainties in parentheses are estimated standard deviations obtained in the least-squares refinements. [a] Other pairs of atoms, not listed here, were also considered in the refinements. These included long-range N · · · C distances between 404 and 524 pm (amplitudes of vibration 18 pm), C · · · C distances in the range 447–730 pm (amplitudes 20–25 pm) and Os · · · H between 323 and 507 pm (amplitudes 15 pm). [b] Fixed.

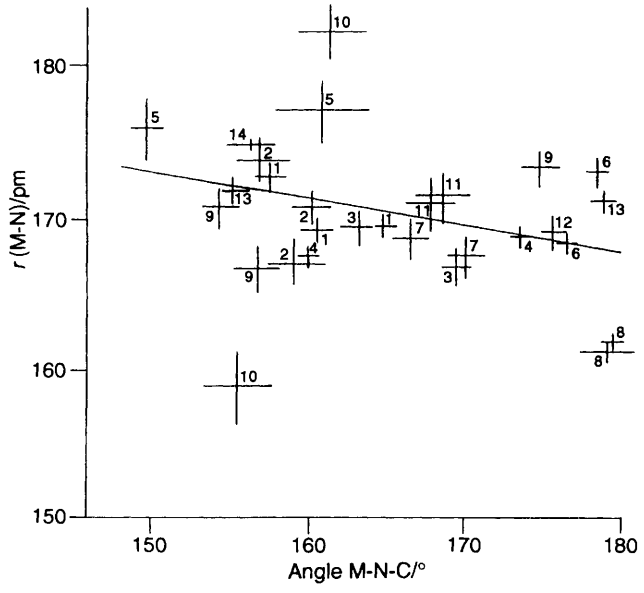

Fig. 4 Correlation of M–N bond lengths and M–N–C angles (showing error bars) for *tert*-butylimido complexes of tungsten, rhenium and osmium.[1,2,12–15] Corrections for the size of the metal atom have been made by subtracting 4.0 pm from W–N and 1.2 pm from Re–N bond lengths. The numbers represent compounds as follows: **1** $Re(OSiMe_3)(NBu^t)_3$;[14] **2** $ReCl(NBu^t)_3$;[14] **3** $ReCl_3(NBu^t)_2$;[14] **4** $ReCl_2Ph(NBu^t)_2$;[14] **5** $Li(tmen)Re(NBu^t)_4$ (tmen = $Me_2NCH_2CH_2NMe_2$);[13] **6** $[Li_2W(NBu^t)_4]_2$;[13] **7** $[W(NBu^t)_2(NH_2Bu^t)Cl(\mu\text{-}Cl)]_2$;[15] **8** $[W_2Cu_5(NBu^t)_2(\mu\text{-}NBu^t)_6(NHBu^t)_2]^+$;[15] **9** $[(Bu^tN)_2Os(\mu\text{-}NBu^t)_2Os(NBu^t)(\mu\text{-}O)]_2$;[2] **10** $[(Bu^tN)_2Os(\mu\text{-}NBu^t)]_2$;[2] **11** $[(Bu^tN)_2Os(\mu\text{-}NBu^t)]_2^{2+}$;[2] **12** $Os(NBu^t)O_3$;[12] **13** $Os(NBu^t)_2O_2$;[1] **14** $Os(NBu^t)_4$

Nitrogen NMR studies of imido complexes[11] have shown that systems having both linear and bent ligands are invariably fluxional, and that chemical shift differences are small. This is consistent with the view that little energy is needed to deform the angle substantially, a view sustained by the wide scatter of data points in Fig. 4. We would therefore expect that the hypothetical linear ligand in $Os(NBu^t)_4$ would have a large-amplitude bending motion, and that as it bent it would be replaced as the linear group by another ligand, in a form of pseudo-rotation. It must be stressed that it is impossible to distinguish this dynamic picture of a molecule with at most C_3 symmetry from the static model with S_4 symmetry from the electron diffraction data. Indeed, even if all four ligands were linear, but undergoing very large-amplitude bending vibrations, the diffraction data would be very similar. In this case the observed S_4 symmetry would imply that the lowest-frequency Os–N–C bending mode of the molecule (which would have T symmetry) would be the triply degenerate t mode. This mode involves motion of pairs of butyl groups [for example, the upper two and the lower two in Fig. 3(*a*)] away from each other. At the same time their associated nitrogen atoms would move towards each other, narrowing the two N–Os–N angles about the remaining C_2 axis. The observed distortion from a regular tetrahedral configuration at the osmium atom can thus easily be rationalised.

Table 5 Structural and spectroscopic data for osmium *tert*-butylimido and oxo complexes

Compound	r(Os–N)/pm	r(Os–O)/pm	OsNC/°	Ref.
$Os(NBu^t)_4$	175.0(3)		156.4(15)	This work
$Os(NBu^t)_2O_2$	171.0(8)	174.4(6)	178.9(9)	1
	171.9(8)		155.1(8)	
$Os(NBu^t)O_3$	168.9(11)	167.7(2)	175.7(7)	12
		169.3(10)		
		171.5(10)		
OsO_4		171.1(3)		8

It would be helpful to compare the structure of $Os(NBu^t)_4$ with those of the isoelectronic ions $Re(NBu^t)_4^-$ and $W(NBu^t)_4^{2-}$. Unfortunately, the rhenium anion has only been studied in the (*N*,*N*,*N*′,*N*′-tetramethylethylenediamine)lithium salt, which has two ligands bridging between lithium and rhenium,[13] and the tungsten anion in its lithium salt, which is a bridged dimer with only one terminal imido ligand per metal atom.[13] This terminal ligand is approximately linear, but both terminal ligands are bent in the rhenium ion. It would be very valuable if structural data could be obtained for these ions in relatively undistorted environments, perhaps by crystallising their $AsPh_4^+$ or $Ph_3PNPPh_3^+$ salts. A study of $Os(NBu^t)O_3$ in the gas phase would also provide useful information about the bending of the butylimido ligand, and allow differences in structural parameters for gaseous and crystalline phases to be assessed.

Molecular Orbital Calculations

Since the geometry of the $Os(NR)_4$ molecule cannot be explained satisfactorily using conventional localised-bonding arguments, it was decided to undertake molecular orbital calculations on $Os(NMe)_4$ and $Os(NH)_4$. The geometries were

Table 6 Structural parameters (°, pm) of optimised structures of $Os(NR)_4$ (R = H or Me)

Complex	Os–N–R	N–Os–N*	N–M–N–R	r(Os–N)	r(N–R)
$Os(NH)_4$	106.2	123.9	12.2	184	103
$Os(NMe)_4$	107.3	154.6	5.1	183	151

* The angle between Os–N bonds related by the C_2 symmetry operation. See Fig. 5.

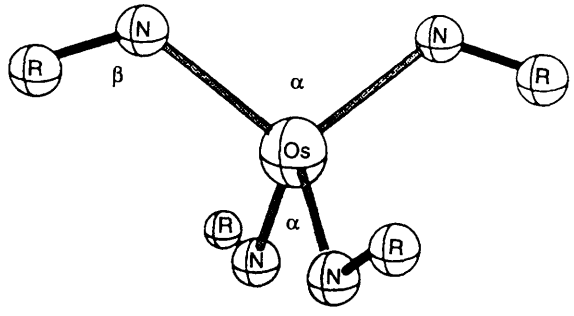

Fig. 5 Optimised structure of the $Os(NR)_4$ complexes

optimised using density functional theory (DFT) molecular orbital calculations as described in the Appendix and interpreted with the assistance of extended-Hückel calculations. The parameters relevant for the latter are also given in the Appendix.[16–26]

The geometries of the $Os(NR)_4$ (R = H or Me) complexes were optimised in C_2 symmetry (see Fig. 5); the resultant geometric parameters are given in Table 6. The molecules were found to have S_4 symmetry and geometries close to that found experimentally. The ligand environment about the metal is pseudo-tetrahedral, with the α and β angles differing slightly from ideal tetrahedral angles. The metal–imide bond angles were calculated to be distinctly non-linear, being 123.9 and 154.6° for the NH and NMe complexes respectively. It should also be noted that there are R–N–Os–N dihedral angles of approximately 12° in the NH complex and approximately 5° in the NMe complex. The dihedral angles are arranged so as to preserve S_4 symmetry. The optimised geometries for the $Os(NR)_4$ molecules are computed to have Os–N distances of 183–184 pm, slightly longer than that determined experimentally (175 pm). This discrepancy is probably due to the omission of any relativistic corrections, which would be expected to improve the accuracy of calculated bond distances. The N–H and N–C bond distances are in excellent agreement with average experimental data.

The electronic structure of $Os(NH)_4$ with T_d symmetry is straightforward. The ligand π orbitals transform as e, t_2 and t_1, of which those of e and t_2 symmetry interact with the metal d orbitals while the t_1 orbitals remain non-bonding because they do not find a symmetry match with the metal orbitals. Distorting the ligand polyhedron to the optimised S_4 structure by bending the N–H or N–C bonds changes the orbital energies. In general the σ orbitals, comprising contributions from s orbitals on the nitrogen atoms, are not greatly affected by this distortion. The π-type orbitals undergo a more substantial change as the symmetry of the ligand polyhedron is reduced. Table 7 shows how the symmetry properties of the π orbitals are changed as a result of the descent in symmetry. Particularly noteworthy is the fact that the interactions between those orbitals derived from the t_1 ligand orbitals and the metal orbitals are no longer symmetry forbidden. The results of the calculations are represented diagrammatically in Fig. 6.

The calculations confirm that the overlap between the metal and the ligand orbitals is stronger in the S_4 case. The main differences are seen to be in the e levels derived from the t_1 orbitals and the b orbital derived from the t_2 set of the tetrahedron. Reducing the symmetry has brought the t_1 orbitals

Table 7 Descent in symmetry of the metal valence and ligand p orbitals from T_d to C_2 symmetry

Orbital*	T_d	S_4	C_2
$(D^{\pi}/\bar{D}^{\pi})_{\pm 1}$	e	a + b	a + a
$P^{\pi}_{0,\pm 1}$	t_2	b + e	a + b + b
$\bar{P}^{\pi}_{0,\pm 1}$	t_1	a + e	a + b + b
s	a_1	a	a
$p_{x,y,z}$	t_2	b + e	a + b + b
d_{z^2}, d_{xy}	e	a + b	a + a
$d_{x^2-y^2}, d_{xz}, d_{yz}$	t_2	b + e	a + b + b

* For an explanation of the notation used to describe the ligand π orbitals above see ref. 27.

Table 8 Electronic energy (kJ mol^{-1}) decomposition for T_d and S_4 geometries

Geometry	E_{a+b}	E_e	E_{total}
T_d	−7 461.4	−7 247.3	−14 708.7
S_4	−7 381.1	−7 428.1	−14 809.2

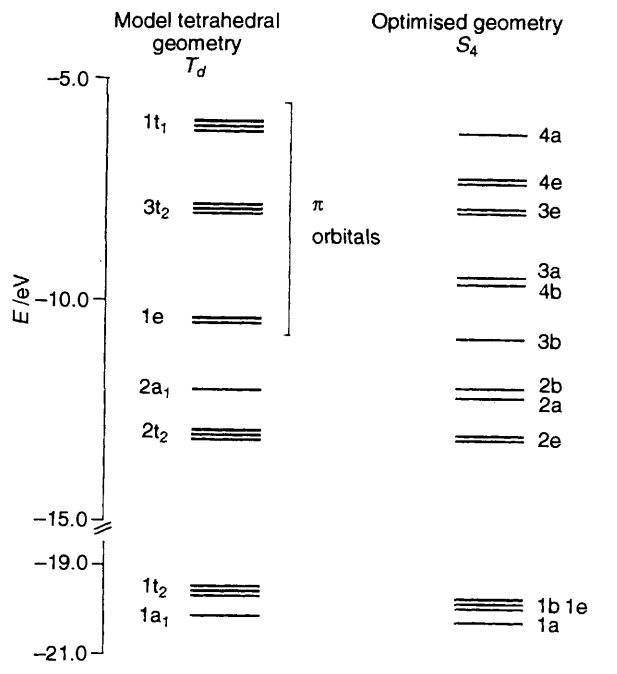

Fig. 6 Comparison of the occupied energy levels of the optimised structure of $Os(NH)_4$ with those of the T_d-restricted compound, obtained using approximate DFT calculations

into play. The overlap between the e component and the d_{xz} and d_{yz} orbitals has resulted in a stabilisation of 125.4 kJ mol^{-1} for these orbitals compared with those of the tetrahedron. In addition, the geometric distortion has resulted in improved overlap between the b component of t_2 and the $d_{x^2-y^2}$ metal orbital.

Employing the transition-state method developed by Ziegler and Rauk,[28] and summarised by equation (A1) in the Appendix, allows the energy changes associated with the a, b and e electronic interactions of the $Os(NH)_4$ complex to be evaluated separately. The respective energies of these interactions are

Table A1

Orbital		H_{ii}/eV	Slater exponent			
Os	6s	−8.0	2.14			
	6p	−4.5	2.10			
N	2s					
	2p					
H	1s					
			ζ_1	c_1	ζ_2	c_2
Os	5d	−12.5	4.29	0.59	1.97	0.58

given in Table 8. The main difference for the alternative geometries is based in the e interactions. For the S_4 geometry the interaction energy for e orbitals is 180.8 kJ mol^{-1} more stabilising than for the tetrahedral complex. This confirms the observations based on the relative overlap populations calculated by the extended-Hückel method. The a and b interactions are seen to be 80.3 kJ mol^{-1} less stabilising in the S_4 complex. Thus by accepting a weakening of nitrogen–hydrogen bonds, in order to capitalise on the increased overlap of the π orbitals with the metal, the complex gains 100.5 kJ mol^{-1} stabilisation.

In conclusion, a distortion from T_d to S_4 symmetry for these molecules results in a greater overlap of the d_{xz} and d_{yz} metal orbitals with the ligand p orbitals. This stabilisation overrides any loss of stabilisation due to reductions in other orbital overlaps. The difference in the metal–imide bond angle between the $Os(NH)_4$ and $Os(NMe)_4$ complexes may be attributed to the different nature of the N–R σ bonds. The s orbital of the hydrogen is less sensitive to angular variation than the sp^3-type orbital of the methyl fragment. This allows for greater flexibility of the metal–imide bond angle for the $Os(NH)_4$ complex.

Appendix

Approximate Density Functional Calculations.—All calculations were based on approximate density functional theory within the local density approximation (LDA).[16] The exchange factor, α_{ex}, was taken as 0.7 and the correlation potential was that of Stoll *et al.*[17] in the parameterisation by Vosko *et al.*[18] The reported calculations were performed utilising the vectorised version of the AMOL program system developed by Baerends *et al.*,[19] and vectorised by Ravenek.[20] The numerical integration procedure applied for the calculations was developed by Boerrigter *et al.*[21] All molecular structures were optimised within the C_2 symmetry group. The geometry-optimisation procedure was based on the method developed by Versluis and Ziegler.[22] A double-ζ-Slater-type orbital (STO) basis set[23] was employed for the *n*s and *n*p shells of the main-group elements. The basis was augmented by a single 3d STO function except for hydrogen, for which a 2p STO was used as polarisation. The n*s*, n*p*, n*d*, (*n* + 1)s and (*n* + 1)p shells of osmium were represented by a triple-ζ-STO basis set.[23] Electrons in lower shells were considered as core and treated according to the method of Baerends *et al.*[19] An auxilliary set[24] of s, p, d, f and g STO functions, centred on all nuclei, was used in order to fit the molecular density and present Coulomb and exchange potentials accurately in each self-consistent field (SCF) cycle. All calculations were spin restricted. Total energies, *E*, were evaluated according to equation (A1). Here E_{HFS} is the

$$E = E_{HFS} + E_c + E_x^{NL} + E_c^{NL} \quad (A1)$$

total statistical energy expression for the Hartree–Fock–Slater method, while E_c, E_x^{NL} and E_c^{NL} are additional correction terms. The first, E_c, is a correlation potential for electrons of different spins in Vosko's parameterisation, the second, E_x^{NL}, is a non-local exchange correction proposed by Becke,[25] and E_c^{NL} is a non-local correction to the correlation, proposed by Perdew.[26]

Extended-Hückel Calculations.—Experimental bond distances were used for these calculations. The atomic parameters used were as in Table A1.

Acknowledgements

We thank the SERC for financial support and for the provision of microdensitometer facilities at the Daresbury Laboratory, and Professor Tom Ziegler, University of Calgary, for the use of his computer facilities.

References

1 W. A. Nugent, R. L. Harlow and R. J. McKinny, *J. Am. Chem. Soc.*, 1979, **101**, 7265.
2 A. A. Danopoulos, G. Wilkinson, B. Hussain-Bates and M. B. Hursthouse, *J. Chem. Soc., Dalton Trans.*, 1991, 269.
3 A. A. Danopoulos, G. Wilkinson, B. Hussain-Bates and M. B. Hursthouse, *J. Chem. Soc., Dalton Trans.*, 1991, 1855.
4 C. M. Huntley, G. S. Laurenson and D. W. H. Rankin, *J. Chem. Soc., Dalton Trans.*, 1980, 954.
5 S. Cradock, J. Koprowski and D. W. H. Rankin, *J. Mol. Struct.*, 1981, **77**, 113.
6 A. S. F. Boyd, G. S. Laurenson and D. W. H. Rankin, *J. Mol. Struct.*, 1981, **71**, 217.
7 A. W. Ross, M. Fink and R. Hilderbrandt, *International Tables for Crystallography*, vol. C, ed. A. J. C. Wilson, Kluwer Academic Publishers, Dordrecht, Boston and London, 1992, p. 245.
8 H. M. Seip and R. Stølevik, *Acta Chem. Scand.*, 1966, **20**, 385.
9 W. A. Herrmann, P. Kiprof, K. Rypdal, J. Tremmel, R. Blom, R. Alberto, J. Behm, R. W. Albach, H. Bock, B. Solouki, J. Mink, D. Lichtenberger and N. E. Gruhn, *J. Am. Chem. Soc.*, 1991, **113**, 6527.
10 W. A. Nugent and J. M. Mayer, *Metal–Ligand Multiple Bonds*, Wiley-Interscience, New York, 1988, ch. 5.
11 D. C. Bradley, S. R. Hodge, J. D. Runnacles, M. Hughes, J. Mason and R. L. Richards, *J. Chem. Soc., Dalton Trans.*, 1992, 1663.
12 B. S. McGilligan, J. Arnold, G. Wilkinson, B. Hussain-Bates and M. B. Hursthouse, *J. Chem. Soc., Dalton Trans.*, 1990, 2465.
13 A. A. Danopoulos, G. Wilkinson, B. Hussain and M. B. Hursthouse, *J. Chem. Soc., Chem. Commun.*, 1989, 896.
14 A. A. Danopoulos, C. J. Longley and G. Wilkinson, *Polyhedron*, 1989, **22**, 2657.
15 A. A. Danopoulos, G. Wilkinson, B. Hussain-Bates and M. B. Hursthouse, *J. Chem. Soc., Dalton Trans.*, 1990, 2753.
16 O. Gunnarsson and I. Lindquist, *Phys. Rev. B*, 1974, **10**, 1319; 1976, **13**, 4274; O. Gunnarsson, M. Johnson and I. Lundquist, *Phys. Rev. B*, 1979, **20**, 3136.
17 H. Stoll, C. M. E. Pavlidou and H. Preuss, *Theor. Chim. Acta*, 1978, **49**, 143; H. Stoll, E. Golka and H. Preuss, *Theor. Chim. Acta*, 1980, **55**, 29.
18 S. J. Vosko, M. Wilk and M. Nusair, *Can. J. Phys.*, 1980, **58**, 1200.
19 E. J. Baerends, D. E. Ellis and P. Ros, *Chem. Phys.*, 1973, **2**, 41.
20 E. J. Baerends, Ph.D. Thesis, Vrije Universitet, Amsterdam, 1975; W. Ravenek, *Algorithms and Applications on Vector and Parallel Computers*, eds. H. J. J. Riele, Th. J. Dekker and H. A. van de Vorse, Elsevier, Amsterdam, 1987.
21 P. M. Boerrigter, G. te Velde and E. J. Baerends, *Int. J. Quantum Chem.*, 1988, **33**, 87.
22 L. Versluis and T. Ziegler, *J. Chem. Phys.*, 1988, **88**, 322.
23 C. J. Snijders, E. J. Baerends and P. Vernooijs, *At. Data Nucl. Data Tables*, 1982, **26**, 483; P. Vernooijs, G. J. Snijders and E. J. Baerends, *Slater Type Basis Functions for the Whole Periodic System*, Internal report, Free University of Amsterdam, 1981.
24 J. Krijn and E. J. Baerends, *Fit Functions in the HFS-method*, Internal report, Free University of Amsterdam, 1984.
25 A. D. Becke, *J. Chem. Phys.*, 1986, **84**, 4524.
26 J. P. Perdew, *Phys. Rev., Lett.*, 1985, **55**, 1655; *Phys. Rev. B*, 1986, **33**, 8822.
27 J. C. Hawes and D. M. P. Mingos, *Struct. Bonding (Berlin)*, 1985, **63**, 1.
28 T. Ziegler and A. Rauk, *Theor. Chim. Acta*, 1977, **44**, 1.

Received 8*th December* 1993; *Paper* 3/07273H